Gaussian Multi-Scale Feature Disassociation Screening in Tuberculosis

Ravi S Malasetty[1], Dr Sanjay Pande[2]
[1]Research scholar, [2]Research supervisor

ABSTRACT
Tuberculosis is a major health threat in many regions of the world. When left undiagnosed and consequently untreated, death rates of patients with tuberculosis are high. We first extract the lung region using a lung nodule Edge detection method. For this lung region, we compute a set of texture and shape features, which enable the x-rays to be classified as normal or abnormal using a binary classifier. Thus, a development of edge detection solution to address these requirements can be implemented in a wide range of situations. The general criteria for edge detection includes detection of edge with lower rorrate ,whichmeans that the detection should accurately catch as many edges.

Keywords: Feature Descriptors, Rotation Variant feature, Tuberculosis

I. INTRODUCTION

Tuberculosis (TB) is the second most common cause of death from an infectious disease worldwide, according to HIV,with a mortality rate of over 1.2 million people in 2010 *[WHO-12]*. TB is an infectious disease. By the bacillus Myco bacterium tuberculosis caused the lung usually It spreads through the air when people with active TB distribute coughing, sneezing or otherwise infectious bacteria. TB in Africa and South east Asia, is wide spread poverty and malnutrition to reduce resistance to the disease most often. In addition, opportunistic infections in immune compromised amplifies the problem of HIV/AIDS patients. *[WHO-11]* The increasing incidence of multi-drug resistant TB was more an urgent need for an in expensive screening technology to have to monitor the progress of treatment. Several antibiotics are available for the treatment of TB.While mortality rate is high, if left untreated, antibiotic treatment improves the chances of survival. In clinical studies, the curerates of over 90% have been documented *[WHO-12]*. Unfortunately, the diagnosis of TB is still a major challenge.

The definitive test for TB is the identification of Myco bacterium tuberculosis in a clinical sputum sample orpus, which is the current gold standard *[WHO-12,GTC-11]*. However, it may take several months to identify these slow-growing organism in the laboratory. Another technique is sputum smear microscopy, in which bacteria in sputum samples are observed under a microscope. This technique was developed more than 100 years ago *[WHO-12]*. In addition, to determine multiple skin tests on the immune response, whether an individual is contracted TB available. Skin tests are not always reliable. The latest development for the detection of molecular diagnostic tests is that are fast and accurate, and are highly sensitive and specific. However, further financial support for these tests to be required common place *[WHO-12, WHO-11, GTC-11]*. In this work, we present an automated approach to detect TB manifest at ions in chest radiographs (CXRS), based on previous work in lung segmentation and lung disease classification *[CJP-12,CPA-13, JKA et.al.,-12]*. An automated approach to reading X-ray allows mass screening of large populations that are not managed manually
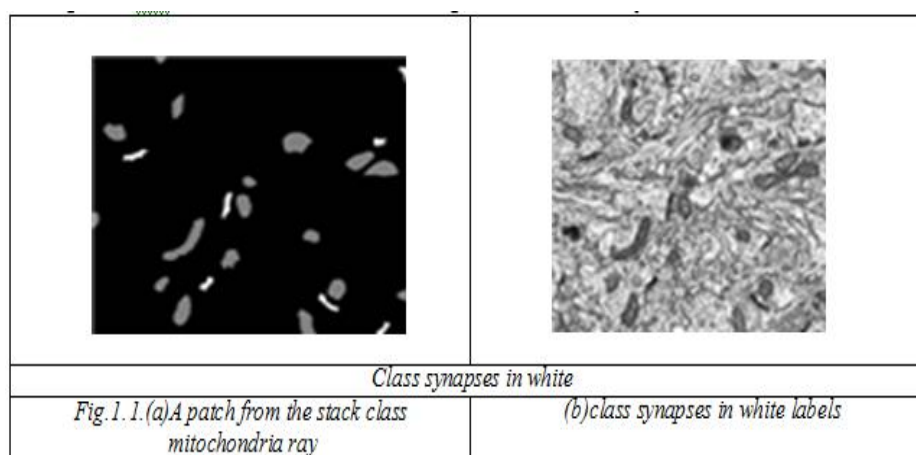
II. LITERATURE SURVEY

Full understanding of the architecture of the brains along term goal of neuroscience. To achieve it, advanced image processing tools are required, that automate the analysis and reconstruction of brain structures. Synapses and mitochondria are two prominent structures with neurological interest for which various automated image segmentation approaches have been recently proposed. In this work we present a comparative study of several image featured escript or used for the segmentation of synapses and mitochondria in stacks of electron microscopy images

Deciphering the architecture of the brain is a key challenge of science [Del-10]. In the last years we have seen advances in the automated acquisition of large series of images of brain tissue [DH-04, KMW et. al.,-08]. The analysis of these images enable the construction of detailed maps of neuron structures from which we will better understand the basic cognitive functions of the brain, such as learning, memory and its pathologies

[KL-10]. There are tools to manually analyze and segment the structures in such images. However, the complexity of these images and the high number of neurons in a small section of the brain, makes the automated analysis the only practical solution.

Mitochondria and synapses are two cell structures of neurological interest that are suitable for automated processing. Synapses are the fundamental mechanism of communication between neurons. Quantification of synapses, and the identification of its types and their distribution is critical to understand how the brain works [BMRet.al.,-13]. Besides providing energy to the cell, mitochondria play an important role in many essential cellular functions including signaling, differentiation, grow than death. The morphology and distribution of Mitochondria has great importance in cellular physiology [CS-10] and synaptic function [LLHet.al.,-07]. Also a typical morphologies or mitochondria distributions are indicative of abnormal cellular states or the existence of neuro degenerative diseases[CNL-10].

Recent works have proposed algorithms for synapse [KSA et.al.,-11] and mitochondria segmentation [GME-12, LSA et.al.,-12] employing various discriminating features. To extract these features some approaches use general texture operators [KSA et.al.,-11], where as others employ specifically designed measurements [LSA et.al.,-12]. In this work, we compare the features used in these works for the problem of joint segmentation of synapses and mitochondria. In Figure6.1,we show a slice of one of the images used in our study and its associated labels.

Class synapses in white

Fig.1.1.(a)A patch from the stack class mitochondria ray	(b)class synapses in white labels

[Bol-79] The traditional methods of classification mainly follow two approaches: unsupervised and supervised. The unsupervised approach attempts spectral grouping that may have an unclear meaning from the user's point of view. Having established these, the analyst then tries to associate an information class with each group. The unsupervised approach is often referred to as clustering and results in statistics that are for spectral, statistical clusters. In the supervised approach to classification, the image analyst supervises the pixel categorization process by specifying to the computer algorithm; numerical descriptors of the various land cover types present in the scene.

*[Pat-72]*Consequently, a prior ground data collection can be very time consuming. Also, the supervised approach is subjective in the sense that the analyst tries to classify information categories, which are often composed of several spectral classes whereas spectrally distinguishable classes will be revealed by the unsupervised approach, and hence ground data collection requirements maybe reduced. Additionally, the unsupervised approach has the potential advantage of revealing discriminable classes unknown from previous work.

Many different aspects of human physiology, chemistry or behavior can be used for biometric authentication. The selection of a particular biometric for use in a specific application involves a weighting of several factors. *[Cha-02]* identified seven such factors to be used when assessing the suitability of any trait for use in biometric authentication. Universality means that every person using a system should possess the trait. Uniqueness means the trait should be sufficiently different for individuals in the relevant population such that they can be distinguished from one another. Permanence relates to the manner in which a trait varies over time. More specifically, a trait with 'good' permanence will be reasonably invariant over time with respect to the specific matching algorithm. Measurability (collectability) relates to the ease of acquisition or measurement of the trait. In addition, acquired data should be in a form that permits subsequent processing and extraction of the relevant feature sets. Performance relates to the accuracy, speed, and robustness of technology used. Acceptability relates to how well individuals in the relevant population accept the technology such that they are willing to have their biometric trait captured and assessed. Circumvention relates to the ease with which a trait might be imitated using an artifact or substitute.

III. METHODOLOGY

Stage 1: Image Registration and Rectification:
Stage 2: Image Enhancement Techniques:
Stage 3: Image Fusion Techniques:
Stage 4: Classification Error Matrix:
Stage 5: Segmentation:
Stage 6: The Parameter Calculation as a criterion for Segmentation:
Stage 7: Neighborhood search-based method to omit isolated noise in the image:
Stage 8: Gabor Filters:
Stage 9: Geometric Methods and Template Matching:

IV. FEATURE DESCRIPTORS

In this section, we describe the feature descriptors considered in this study. We begin describing the simple general purpose descriptors and proceed in order of increasing sophistication.

A. Simple Window and Histogram: We construct a simple window based descriptor ordering and storing a vector of then $\times$ n neighborhood of the pixel that we want to describe. This naïve descriptor has proved to be an excellent source of information for texture segmentation *[VZ-03]*. A histogram based descriptor takes for each pixel an n$\times$n neighborhood on which a gray level histogram is computed. In *[LSA et.al.,-12]*, a histogram and the Ray features *[SCL-09]* are used as elements of the feature vector form it ochondria segmentation. In this wealso tested the histogram and the ray features separately.

B. Local Binary Patterns: The local binary patterns (LBP)*[OPH-96]*,generate a binary code with k digits taking in to account for each pixel pase to f k neighbor points at an **r** distance, wherer is the radius from the central pixel p to its neighbors. If the value of p is higher than a neighbor k_i then we insert a O In the binary code, or 1ift he value is lower. The feature vectoris obtained from the histogram of the LBP binary codes converted to its real values in an$\times$n neighborhood. This process is out lined in *Figure2*.
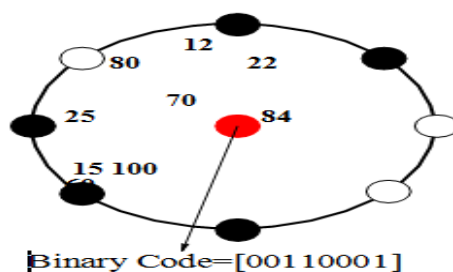

Figure2. Computing Pixel Values of neighboring pixels:

Depending on the values of the neighboring pixels, the LBP generates a binary code that can be converted to a real value. In this case the value would be: $0\times1+0\times2+1\times4+1\times8+0\times16+0\times32+0\times64+1\times128 = 148$.

C. GRIMS: The GRIMS (Gaussian Rotation In variant and Multi-Scale) descriptors apply to each image in the stack a set of linear Gaussian filters at different scales to compute zero, first and second order derivatives. These linear operators are:
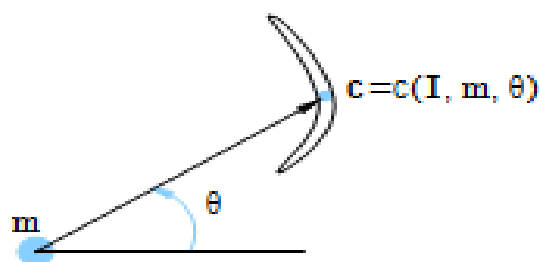

Figure 3. Illustration of Nearest Contour

Function c returns the position c from the nearest edge or cont our of the image **I** to the position m in direction defined by the angleθ.

$$G\sigma *, \sigma \cdot G\sigma * \frac{\partial}{\partial x} \sigma \cdot G\sigma * \frac{\partial}{\partial y} \sigma 2 * G\sigma \frac{\partial 2}{\partial x2} G\sigma * \frac{2}{\partial xy} \sigma * \partial y2 \qquad (6.1)$$

WhereGσ is a Gaussian filter with standard deviation σ and * is the convolution operator. We will call the result of applying these operators to the image: s00, s10, s01, s20, s11 and s02, where the subscript denotes the order of the derivatives.

The feature vector calculated for each pixel in the image at scale σ is

$$\lambda 1 = \tfrac{1}{2} * s20 + s02 + \frac{q}{(s20 - s02)2 + 4s11}(6.2)$$

$$\lambda 2 = \tfrac{1}{2} * s20 + s02 - \frac{q}{(s20 - s02)2 + 4s11}(6.3)$$

s00, s10 + s01, λ1, λ2, where s10 + s01 is the gradient magnitude and λ1 y λ2 are the eigen values of the Hessian matrix calculated as follows:

This procedure is repeated with various scales σ0,...,σn−1, and since there are 4 features for each scale, we obtain a feature vector of size 4n. In our experiments we use n = 4 scales, therefore, we obtain a feature vector with 16 dimensions.

V. EXPERIMENTATION

We used an image stack obtained from the somatosensory cortex of a rat, with a resolution of 3.686μm per pixel. The thickness of each layer is 20μm. We used 60 images of the stack for training and 10 for testing. The related outcome of the computation is personated in *Figure 6.4*.

Forthedescriptors that use a Gaussian kernel, we experimentally selected the scales σ0 = 4,σ1 = 5.65,σ2 = 8,σ3 = 11.31,σ4 = 16 for our tests. In our HOG implementation we used 4×4 pixels per cell and 6×6 cells per block. Due to the block division required, we assigned the computed histogram to the central pixel in each cell.

For the histogram and simple window descriptors, we tested with several window and bin sizes. A 20 × 20 pixel window with 10 bins for the histogram and a 15×15 box for the simple window had the best performance.

For the LBP we use the radius of 10 pixels with 25 sample points from which we obtain the LBP code for each pixel. With such codification we obtain a new image stack on which we compute a 10 bins histogram on a 20×20 pixels window, from which we build our feature vector.
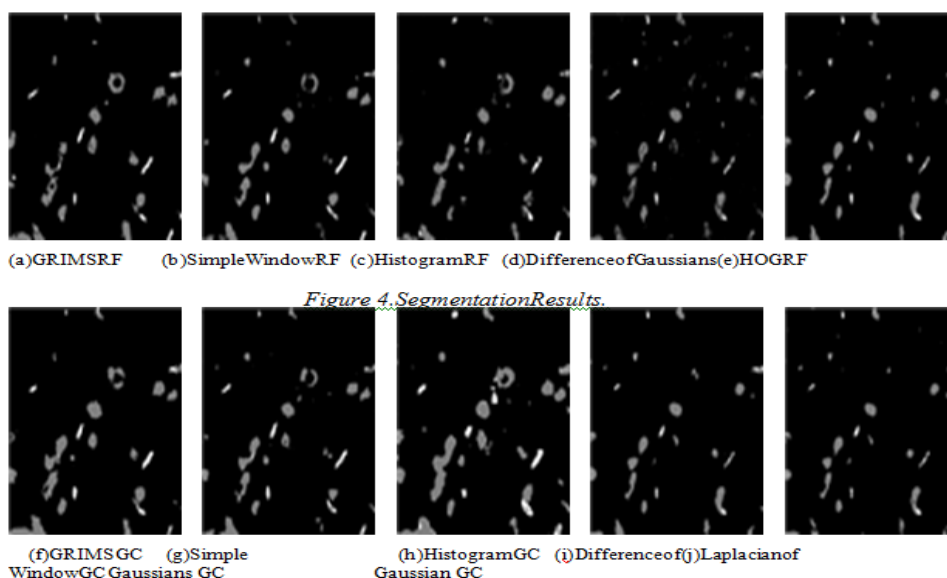
(a)GRIMSRF   (b)SimpleWindowRF   (c)HistogramRF   (d)DifferenceofGaussians(e)HOGRF

Figure 4.SegmentationResults.

(f)GRIMSGC   (g)Simple WindowGC Gaussians GC   (h)HistogramGC   (i)Differenceof(j)Laplacianof Gaussian GC

In the first row the best results with Random Forest Classifier and in these cond row the best results with Gaussian Classifier For classification purposes we used two algorithms. A Gaussian and a Random Forest Classifier.

The Gaussian classifier is a generative parametric classifier that assumes Gaussian class conditional distributions. We chose this classifier because of its simplicity and speed. Random forests operate by training a multitude of decision trees and selecting the class label that is the mode of the classes output by individual trees. We used the scikit-learn *[PVG et.al.,-11]*implementation of the Random Forest classifier with 100 decision trees.

Thehighdimensionalityofthefeaturevectorsproducedbythe HOGandRadon-Likefeaturedescriptors,giventhe numberoftrainingsamples, producedgenerateGaussiandistributionswithsingularcovariancematrices.Forthisreasoninourexperimentswedo notuseaGaussianclassifierwithHOGandRadon-Likefeatures.Similarly,wedonotshowtheresultsoftheRandomForestclassifierwithLBPfeatures,givenitspoorper formance.

In our experiments we use the ROC curve of each class against there stand the Jaccard Index as comparison indices. We have performed an extensive set of experiments involving different feature configuration. We compared our work with the Radon-Like features *[KVP-10]* and the work in *[LSA et.al.,-12]* but testing the descriptors of their feature vector individually, i.e., the histogram and Ray descriptors were tested separately. The results of our experiments show that the Random Forest classifier achieves the best performance for both mitochondria and synapse segmentation. However, as shown in *Table1.0*, the time it takes to train and classify is roughly one order of magnitude larger than the Gaussian classifier. On the other hand, the Gaussian Classifier is significantly faster than the Random Forest at expense of a margin al loss in performance.

The GRIMS descriptors provide the best performance for mitochondria segmentation, closely followed by the simple window. On the other hand, for the segmentation of synapses, the simple window descriptor provides the best performance, immediately a head of the GRIMS.

Descriptor	Learning	Prediction
Random Forest Classifier		
LBP	27.0 min	36.0s
Simple Window	126.1min	29.4s
Histogram	12.3min	13.29s
GRIMS	35.2min	15.54s
Ray	53.1min	19.0s
HOG	54.4min	21.0s
Laplacian of Gaussian	18.4min	11.3s
Difference of Gaussians	18.6min	11.9s
Gaussian Classifier		
LBP	1.4s	1.3s
Simple Window	3.0s	1.2s
Histogram	3.0s	0.5s
GRIMS	1.2s	1.0s
Ray	2.0s	0.4s
Eigen values of Structure Tensor	2.1s	0.2s
Laplacian of Gaussian	2.3s	1.0s
Difference of Gaussians	2.3s	1.1s

Table 1.0: Learning and Prediction in Classifiers

VI.   SUMMARY
Edge detection, especially step edge detection has been widely applied in various different computer vision systems, which is an important technique to extract useful structural information from different vision objects and dramatically reduce the amount of data to be processed. It was found that, the requirements for the application of edge detectionon diverse vision systems are relatively the same.
We tested nine feature descriptors with two classifiers in an EM stack for the joint segmentation of mitochondria and synapses. Our results show that GRIMS and simple window descriptors exhibit the best performance. Although the Random Forest classifier achieves better precision, we suggest the use of the Gaussian Classifier given the large size of the typical EM image stacks and the gains in speed provided by this classifier.

Thus anautomated system for CXRS manifestations of TB screens.The system is currently set for practical use,where they are part of a mobile system for TB screening in remote areas. When the CXR as input, our system first segments the lung area with an optimization method based on Canny edge detection. This method combines intensity information with personalized lungs At las models derived from the training set. We calculate a set of shape, edge and texture features as input a binary classifier, then classifies the input image in to a predetermined either normal or abnormal.

REFERENCES

[1]. [BMR et.al.,-13]L. Blazquez-Llorca, A. Merchan-Perez, J. R. Rodrıguez, J. Gascon, and J. DeFelipe, "FIB/SEM technology and alzheimer's disease: Three-dimensional analysis of human cortical synapses," Journal of Alzheimer's Disease, vol. 34, no. 4, pp. 995–1013, 2013.

[2]. [Bol-79]Bolles, Robert; Learning Theory ; Holt , Rinchart and Winston, New York 1979

[3]. [Cha-02] M. S. Charikar. "Similarity Estimation Techniques from Rounding Algorithms". In Proceedings of the 34th Annual ACM Symposium on Theory of Computing, 2002.

[4]. [CJP et.al.,12] S. Candemir, S. Jaeger, K. Palaniappan, S. Antani, and G. Thoma, "Graph-cut based automatic lung boundary detection in chest radiographs," in Proc. IEEE Healthcare Technol. Conf.: Translate. Eng. Health Med., 2012, pp. 31–34.

[5]. [CNL-10] D.-H. Cho, T. Nakamura, and S. Lipton, "Mitochondrial dynamics in cell death and neurodegeneration," Cellular and Molecular Life Sciences, vol. 67, no. 20, pp. 3435–3447, 2010.

[6]. [CPA-13] S. Candemir, K. Palaniappan, and Y. Akgul, "Multi-class regularization parameter learning for graph cut image segmentation," in International Symposium on Biomedical Imaging, 2013, pp. 1473–1476.

[7]. [CS-00] Cristianini, N. and Shawe-Taylor, J. (2000). An introduction to Support Vector Machines and other kernel-based learning methods. Cambridge University Press, Cambridge, UK.

[8]. [Del-10] J. DeFelipe, "From the connectome to the synaptome: An epic love story," Science, vol. 330, no. 6008, pp. 1198–1201, 2010.

[9]. [DH-04] W. Denk and H. Horstmann, "Serial block-face scanning electron microscopy to reconstruct three-dimensional tissue nanostructure," PLoS Biol, vol. 2, no. 11, p. e329, 10 2004.

[10]. [GME-12] R. Giuly, M. Martone, and M. Ellisman, "Method: automatic segmentation of mitochondria utilizing patch classification, contour pair classification, and automatically seeded level sets," BMC Bioinformatics, vol. 13, no. 1, p. 29, 2012.

[11]. [GTC-11] Global Tuberculosis Control 2011. World Health Organization, 2011.

[12]. [JKA et.al.,-12] S. Jaeger, A. Karargyris, S. Antani, and G. Thoma, "Detecting tuberculosis in radiographs using combined lung masks," in Int. Conf. IEEE Engineering in Medicine and Biology Society (EMBS), 2012, pp. 4978– 4981.

[13]. [KL-10] N. Kasthuri and J. W. Lichtman, "Neurocartography," Neuropsy-chopharmacology, 2010.

[14]. [KMWet.al.,-08] G. Knott, H. Marchman, D. Wall, and B. Lich, "Serial section scanning electron microscopy of adult brain tissue using focused ion beam milling," Journal of Neuroscience, vol. 28, no. 12, pp. 2959–2964, 2008.

[15]. [KSS et.al.,-11] A. Kreshuk, C. N. Straehle, C. Sommer, U. Koethe, M. Cantoni, G. Knott, and F. A. Hamprecht, "Automated detection and segmentation of synaptic contacts in nearly isotropic serial electron microscopy images," PLoS ONE, vol. 6, no. 10, p. e24899, 10 2011.

[16]. [LLH et.al.,-07] D. Lee, K.-H. Lee, W.-K. Ho, and S.-H. Lee, "Target cell-specific involvement of presynaptic mitochondria in post-tetanic potentiation at hippocampal mossy fiber synapses," The Journal of Neuroscience, 2007.

[17]. [LSA et.al.,-12] A. Lucchi, K. Smith, R. Achanta, G. Knott, and P. Fua, "Supervoxel-based segmentation of mitochondria in em image stacks with learned shape features," IEEE Transactions on Medical Imaging, vol. 31, no. 2, pp. 474–486, 2012.

[18]. [OPH-96] T. Ojala, M. Pietikainen, and D. Harwood, "A comparative study of texture measures with classification based on featured distributions," Pattern recognition, vol. 29, no. 1, pp. 51–59, 1996.

[19]. [Pat-72] E.A. Patrick, Fundamentals of Pattern Recognition, Prentice Hall, Inc, N.J.,1972.

[20]. [PVG et.al.,-11] F. Pedregosa, G. Varoquaux, A. Gramfort, V. Michel, B. Thirion, O. Grisel, M. Blondel, P. Prettenhofer, R. Weiss, V. Dubourg, J. Vander-plas, A. Passos, D. Cournapeau, M. Brucher, M. Perrot, and E. Duch-esnay, "Scikit-learn: Machine learning in Python," Journal of Machine Learning Research, vol. 12, pp. 2825–2830, 2011.

[21]. [SCL-09] K. Smith, A. Carleton, and V. Lepetit, "Fast ray features for learning irregular shapes," in Proc. Int. Conference on Computer Vision, 2009, pp. 397–404.

[22]. [VZ-03] M. Varma and A. Zisserman, "Texture classification: Are filter banks necessary?" in IEEE Conference on Computer Vision and Pattern Recognition, vol. 2, 2003, pp. 691–698.

[23]. [WHO-11] Stop TB Partnership, The Global Plan to Stop TB 2011-2015. World Health Organization, 2011.

[24]. [WHO-12] WHO, Global Tuberculosis Report. World Health Organization, 2012.